A&A 495, 147–155 (2009)
DOI: 10.1051/0004-6361/200809886

Astronomy & Astrophysics

No evidence of mass segregation in massive young clusters

J. Ascenso[1,2], J. Alves[3], and M. T. V. T. Lago[1,4]

[1] Centro de Astrofísica da Universidade do Porto, Rua das Estrelas, 4150-762 Porto, Portugal
e-mail: jascenso@astro.up.pt
[2] Harvard-Smithsonian Center for Astrophysics, 60 Garden Street, Cambridge, MA 02138, USA
[3] Calar Alto Observatory – Centro Astronómico Hispano-Alemán, C/ Jesús Durbán Remón 2-2, 04004 Almeria, Spain
[4] Departamento de Matemática Aplicada da Faculdade de Ciências, Universidade do Porto, Rua do Campo Alegre, 657, 4169-007 Porto, Portugal

Received 1 April 2008 / Accepted 17 November 2008

ABSTRACT

Aims. We investigate the validity of the mass segregation indicators commonly used in analysing young stellar clusters.
Methods. We simulate observations by constructing synthetic seeing-limited images of a 1000 massive clusters (10^4 $M_\odot$) with a standard IMF and a King-density distribution function.
Results. We find that commonly used indicators are highly sensitive to sample incompleteness in observational data and that radial completeness determinations do not provide satisfactory corrections, rendering the studies of radial properties highly uncertain. On the other hand, we find that, under certain conditions, the global completeness can be estimated accurately, allowing for the correction of the global luminosity and mass functions of the cluster.
Conclusions. We argue that there is currently no observational evidence of mass segregation in young compact clusters since there is no robust way to differentiate between true mass segregation and sample incompleteness effects. Caution should then be exercised when interpreting results from observations as evidence of mass segregation.

Key words. open clusters and associations: general – methods: statistical

1. Introduction

The issue of mass segregation in globular and open clusters has been discussed in the literature for over 20 years. Historically, the first indicator of mass segregation was simply that the brightest, most massive cluster members lay closest to the cluster core, whereas the faintest, lower-mass members fill the whole extent of the cluster area (McNamara & Sekiguchi 1986, and references therein). The mass segregation issue has since been complemented with specific properties that overall quantify the differences in the spatial distribution of high- and low-mass stars. The most commonly used for this effect are: (1) the radial dependence of the mass function (e.g., Moitinho et al. 1997; Stolte et al. 2006; Schweizer 2004; Gouliermis et al. 2004) or luminosity function (e.g., Jones & Stauffer 1991; de Grijs et al. 2002); (2) the radial differences in the ratio of high- to low-mass stars (e.g., Hillenbrand 1997); (3) the mean mass within some characteristic radius (e.g., Sagar et al. 1988; Hillenbrand & Hartmann 1998); and (4) the mean radius of the two distributions (e.g., Sagar et al. 1988; de Grijs et al. 2002) or the direct comparison of the cumulative radial density distribution for the two subsamples (e.g., McNamara & Sekiguchi 1986; Tadross 2005).

Even though almost all young clusters present one or more of these properties, several authors have shown that the timescale for dynamical relaxation is typically longer than the clusters' age (e.g., Bonnell & Davies 1998), implying that the observed mass segregation should not be dynamical in origin. Faster phenomena, such as violent relaxation (Hillenbrand & Hartmann 1998; Binney & Tremaine 1987) and the fact that the massive stars have shorter relaxation times (Hillenbrand & Hartmann 1998, and references therein) still do not seem to be sufficient for explaining the profusion of young clusters presenting these properties or the implicit degree of mass segregation. The alternative is a primordial origin, in which the distribution of massive stars in young clusters must reflect the initial conditions and the processes involved in cluster formation (e.g., Bonnell 2000).

Conversely, some authors have indirectly shown that the way some indicators are presented is not statistically accurate. For example, Maíz Apellániz & Úbeda (2005) prove that a significant bias is introduced when building the mass function in equal $\Delta \log(M/M_\odot)$ bins, as is done in the literature. A statistical bias is also potentially introduced when studying the radial properties of a cluster by dividing the cluster area in fixed-width or constant-area annuli rather than equal-number annuli, as each annulus will contain different numbers of stars changing the statistical significance from one annulus to the next.

In this paper we propose to investigate the validity of a few traditional mass segregation indicators using synthetic, 10^4 $M_\odot$-class clusters. We describe the biases that result directly from the binning of the data and then explore the incompleteness in observed samples and its consequences on the mass segregation indicators.

The nomenclature used throughout the text is summarised as follows:

True clusters: synthetic clusters (Sect. 2.1).
Observed clusters*: synthetic observations (Sect. 2.2).
Completeness tests: completeness assessment obtained by adding artificial stars of increasing magnitude to the cluster image in a grid. Derived completeness is defined as the number of detected grid stars with measured magnitudes $m_{\rm out}$ that satisfy the condition $|m_{\rm out} - m_{\rm in}| < 0.1$, divided by the total number of

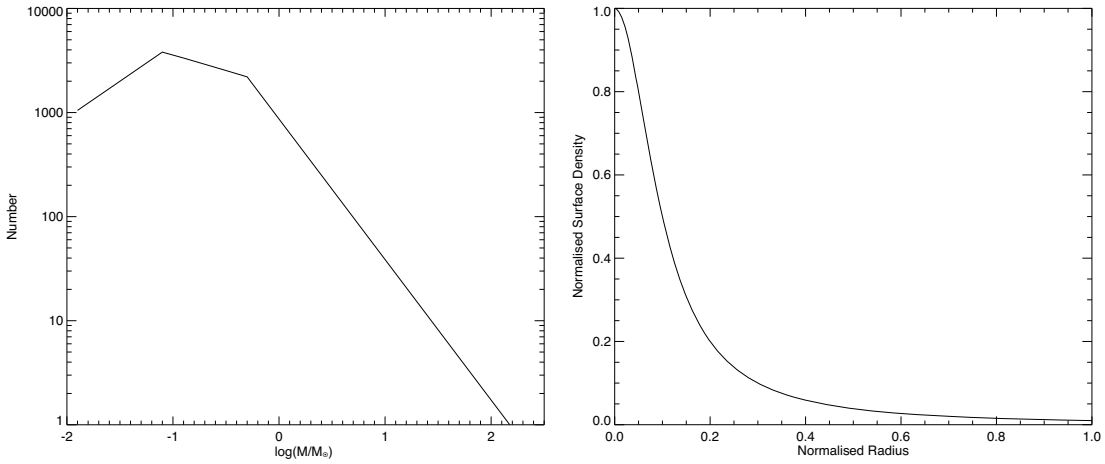

Fig. 1. *Left*: Salpeter (1955) ($M > 0.5\ M_\odot$) and Kroupa (2001) ($M \leq 0.5\ M_\odot$) mass function used to generate the synthetic clusters. *Right*: normalized King (1962) surface density profile.

stars of magnitude $m_{\rm in}$ in the input grid (Sect. 4.1). This would be the assessment an observer could do in real data.
True completeness: completeness assessment obtained by direct comparison of the observed* and true clusters. Derived completeness is defined as the number of stars in the observed* cluster divided by the corresponding number of stars in the true cluster (Sect. 4.2). This assessment is only possible because we know the true composition of the cluster.

2. Simulations

2.1. Synthetic clusters

We created 1000 synthetic clusters, each containing 2×10^4 stars (total mass of $1.5\times10^4\ M_\odot$). Each cluster member was assigned a mass from a Salpeter (1955) ($M > 0.5\ M_\odot$) and Kroupa (2001) ($0.01\ M_\odot \leq M \leq 0.5\ M_\odot$) IMF (Fig. 1, *left*):

$$\Gamma = \frac{{\rm d}\log N}{{\rm d}\log M} = \begin{cases} -1.35 & 0.5 \leq M/M_\odot \\ -0.3 & 0.08 \leq M/M_\odot < 0.5 \\ +0.7 & 0.01 \leq M/M_\odot < 0.08. \end{cases} \quad (1)$$

The radial position (distance to the centre) of each artificial star was drawn randomly and *independently of mass* from a King (1962) radial surface density profile (Fig. 1, *right*):

$$\Sigma(r) = \frac{\Sigma_0}{1 + (r/r_{\rm c})^2} \quad (2)$$

with a core radius $r_{\rm c}$ of 0.2 pc, using the Monte Carlo method of the cumulative distribution function. For a cluster of 2×10^4 stars, this yields a central projected density Σ_0 around 10^4 pc^{-2}. In this way the synthetic clusters are blind to any correlation between position and mass, i.e., they are not mass segregated. We have not set any boundary conditions regarding the physics of star formation or dynamical evolution, except for the underlying assumption that the probability distribution function from which the positions and masses are drawn are a King profile and a Kroupa-Salpeter IMF. We have also not set any high mass cutoff.

2.2. Synthetic observations

To investigate the impact of incompleteness due to crowding – a strong limitation in most studies of mass segregation in real (massive) clusters – we have used IRAF mkobject to build "seeing limited" images of the synthetic clusters. The masses were transformed into K-band luminosities using the mass-luminosity relation from Ascenso et al. (2007) for a distance of 3 kpc and no interstellar extinction. This configuration produced stars up to magnitude 19. Since the Monte Carlo algorithm for the positions only generates the r polar coordinates, a value for θ was assigned to each r from a uniform random distribution between 0 and 360°. Figure 2 shows three of the clusters obtained in this way.

These images were treated as actually observed clusters, in the sense that they were subjected to a source extraction algorithm (IRAF daofind), PSF photometry (IRAF allstar), and cuts in photometric errors to produce the final samples. These synthetic observations were only sensitive to stars up to magnitude 16.5, with only ~29% of the original sources up to this magnitude being detected. The 1000 catalogues produced in this way are hence incomplete sub-samples of the original synthetic clusters. Since they are meant to pose as real observations, we will hereafter refer to the (incomplete) sub-samples as *observed**, always maintaining the asterisk to avoid confusion with actual observations that are not presented here. The properties of the (complete) clusters originally generated by the simulations will be labeled as *"true"*, since they refer to all the stars.

3. Results

We tested the most commonly used mass segregation indicators on synthetic, non-segregated clusters to investigate how the way we approach observational data may influence our perception of mass segregation in massive clusters.

For each indicator we investigate: (1) the results expected for a non-segregated cluster; (2) the statistical effects of binning; and (3) the effects of incompleteness of the sample due to crowding. The first item is measured directly from the synthetic clusters and averaged over the whole set to produce the expected properties of a "perfect cluster". The second concerns the way the quantities are represented and how it may affect the analysis. The third is measured on the observed* clusters to explore in which ways the incompleteness of the observed samples due to crowding can mimic the effects of mass segregation.

We used the full width at half maximum of the stars in the simulated observations (5 pixels) as the (arbitrary) unit of length.

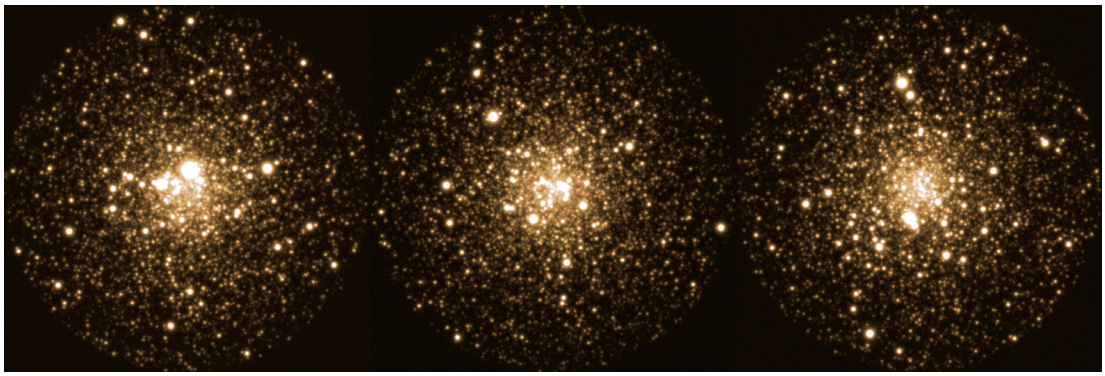

Fig. 2. Seeing limited images of three simulated clusters. The brightness of the sources corresponds to the *K*-band.

3.1. Slope vs. radius

The variation of the mass function (MF) with radius is already a traditional diagnosis tool for mass segregation (Moitinho et al. 1997; de Grijs et al. 2002; Stolte et al. 2002; Gouliermis et al. 2004; Bonatto & Bica 2005; Stolte et al. 2005; Bica & Bonatto 2005). In a mass segregated cluster we expect to find an increase in the number of massive stars with respect to the number of low-mass stars toward the centre, which translates into a flattening of the mass function or an increase of the high-mass end slope, hereafter referred simply as slope or Γ. Conversely, in a non-segregated cluster we expect the slope to be constant with radius.

3.1.1. Binning effects

This section discusses the MF slope analysis performed on the original 2×10^4-star clusters.

When investigating the radial dependence of the mass function we must bin the data twice: first we divide the cluster area into concentric annuli and then bin the masses of the objects in each annulus to produce the mass function for that annulus. In order to keep the statistical significance and avoid biases, these bins should be defined such as to keep the number of stars per bin constant. Historically, the radial bins are defined as fixed-width or fixed-area annuli, whereas the mass bins are defined from the histogram of $\log(M/M_\odot)$, as constant $\Delta\log(M/M_\odot)$ bins, neither one keeping the number of stars per bin constant. Instead, the radial bins should be defined as equal-number annuli, and the mass function as a histogram with each bin containing the same number of stars and divided by the resultant bin width (Maíz Apellániz & Úbeda 2005).

Figure 3 shows the variation of Γ with radius for the 1000 synthetic 2×10^4-star clusters, calculated with several combinations of radial and mass bins. The three panels to the left have the masses appropriately binned, according to Maíz Apellániz & Úbeda (2005), whereas the panels to the right are produced using the more traditional mass functions from fixed $\Delta\log(M/M_\odot) = 0.2$ histograms of $\log(M/M_\odot)$. In the two top panels the radii are binned in annuli with equal number (100) of stars, the middle panels have fixed-width (10 FWHM) radial annuli, and in the bottom panels the slope of the MF is measured (cumulatively) in circles.

The profile in *panel a)* is unbiased since we guarantee the same statistical significance in both the radial and the mass bins by keeping the number of stars in each bin constant. As such, we find that Γ is constant with radius, as expected for non-segregated clusters, and equal to the input value for the simulations, −1.35. When we change the statistical significance of the radial bins by considering fixed-width annuli (*panel b)*) or circles (*panel c)*) while keeping the statistical significance of the mass bins, we still find the behaviour expected of non-segregated clusters.

Conversely, all panels to the right display odd trends not reflecting the conditions set for the simulations. *Panel d)* presents a Γ that is constant with radius, hence not suggesting mass segregation, but larger than the input value of −1.35, illustrating the intrinsic bias in characterising a MF built from fixed $\Delta\log(M/M_\odot)$ bins (Maíz Apellániz & Úbeda 2005). In *panels e)* and *f)* this bias conspires to produce contradictory behaviours: *panel e)* shows a flattening of the MF outward, whereas *panel f)* shows a flattening of the MF inward. The profile in *panel f)* is what we would expect to find in a mass-segregated cluster, although it only appears as a consequence of the mass binning. Furthermore, as can be seen from the last bin, the overall mass function of the cluster as measured in fixed $\Delta\log(M/M_\odot)$ bins comes out shallower than Salpeter, revealing a fundamental underlying bias in this representation of the mass function, as we built the clusters to be Salpeter in the first place.

This shows that the mass function slope is robust against radial binning, only if the mass function itself is built in an unbiased way, namely using the Maíz Apellániz & Úbeda (2005) method to bin the masses.

3.1.2. Incompleteness effects

The effects of incompleteness on the radial distribution of the mass function slope were tested on the observed* clusters. The completeness assessment and tentative corrections will be addressed in Sect. 4. Figure 4 shows the radial dependence of Γ for these clusters using the same binning combinations as described above. The *light lines* correspond to the radial profiles for the "true" clusters from Fig. 3.

In all panels, regardless of the binning in radius or mass, we find a flattening of the MF toward the centre of the cluster, a signature typically attributed to mass segregation. These profiles are in all similar to those described in the literature as indicative of mass segregation (e.g., Brandl et al. 1996; Stolte et al. 2002, 2006; Schweizer 2004; Gouliermis et al. 2004; Bonatto & Bica 2005). In our case, since we know the "true" clusters are not segregated, the finding of this signature in the observed* clusters cannot be regarded as evidence of mass segregation in the underlying cluster, but rather as a consequence of crowding. In the presence of incompleteness, the statistical biases arising from binning are largely overcome by the fact that the low-mass stars go undetected in the cluster core. The mass-binning effects are only observed as a flatter mass function in general.

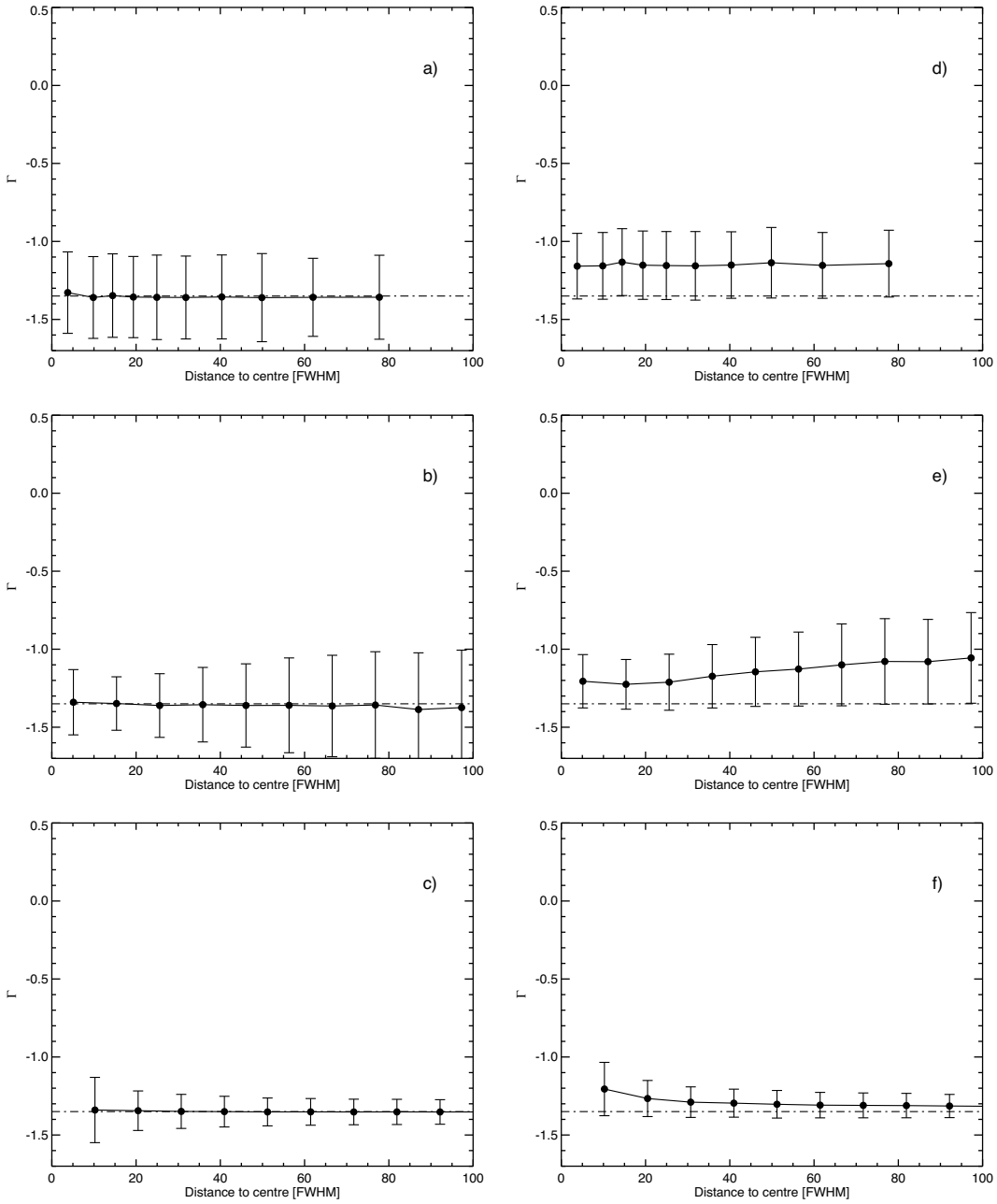

Fig. 3. Mass function slope (Γ) as a function of radius for the synthetic clusters. Panel **a)**: Γ is measured in equal-number (100 stars) radial annuli (the radii mark the centre of the annuli) and defining the mass functions such that all the mass bins have the same number of stars. Panel **b)**: Γ is measured in fixed-width (10 FWHM) radial annuli (the radii mark the centre of the annuli) and defining the mass function as in panel a). Panel **c)**: Γ is measured in concentric circles (the radii mark the limits of the circles) and defining the mass function as in panel a). Panel **d)**: Γ is measured in equal-number (100 stars) radial annuli and defining the mass functions as fixed $\Delta \log(M/M_{\odot})$ histograms. Panel **e)**: Γ is measured in fixed-width (10 FWHM) radial annuli and defining the mass function as in panel **d)**. Panel **f)**: Γ is measured in concentric circles and defining the mass function as in panel **d)**.

3.2. Ratio of high- to low-mass stars

In any given region of a non-segregated cluster, apart from fluctuations, there should be the same proportion of high and low-mass objects as imposed by the underlying mass function. In particular, the ratio of high- to low-mass stars should not be dependent on radius. This is indeed what we find for the synthetic clusters, regardless of how we divide the cluster radially. The *light symbols* in Fig. 5 show this profile for a high-mass/low-mass threshold of 10 $M_{\odot}$, and radial binning consisting of equal-number annuli (*left-hand panel*), fixed-width annuli (*middle panel*), and concentric circles (*right-hand panel*). All the profiles are flat, again validating the absence of mass segregation in the synthetic clusters, and present no signature of statistical biases arising from radial binning effects.

The *dark symbols* in the panels show the variation of the ratio of high- to low-mass stars in the observed* clusters. For all geometries the ratio increases toward the cluster core, suggesting an apparent depletion of low-mass stars in the core. This is a direct consequence of crowding that does not allow for the effective detection of faint sources, rather than an actual absence of low-mass stars in the underlying cluster that could be imputed to mass segregation. Again, this profile is similar to those cited in

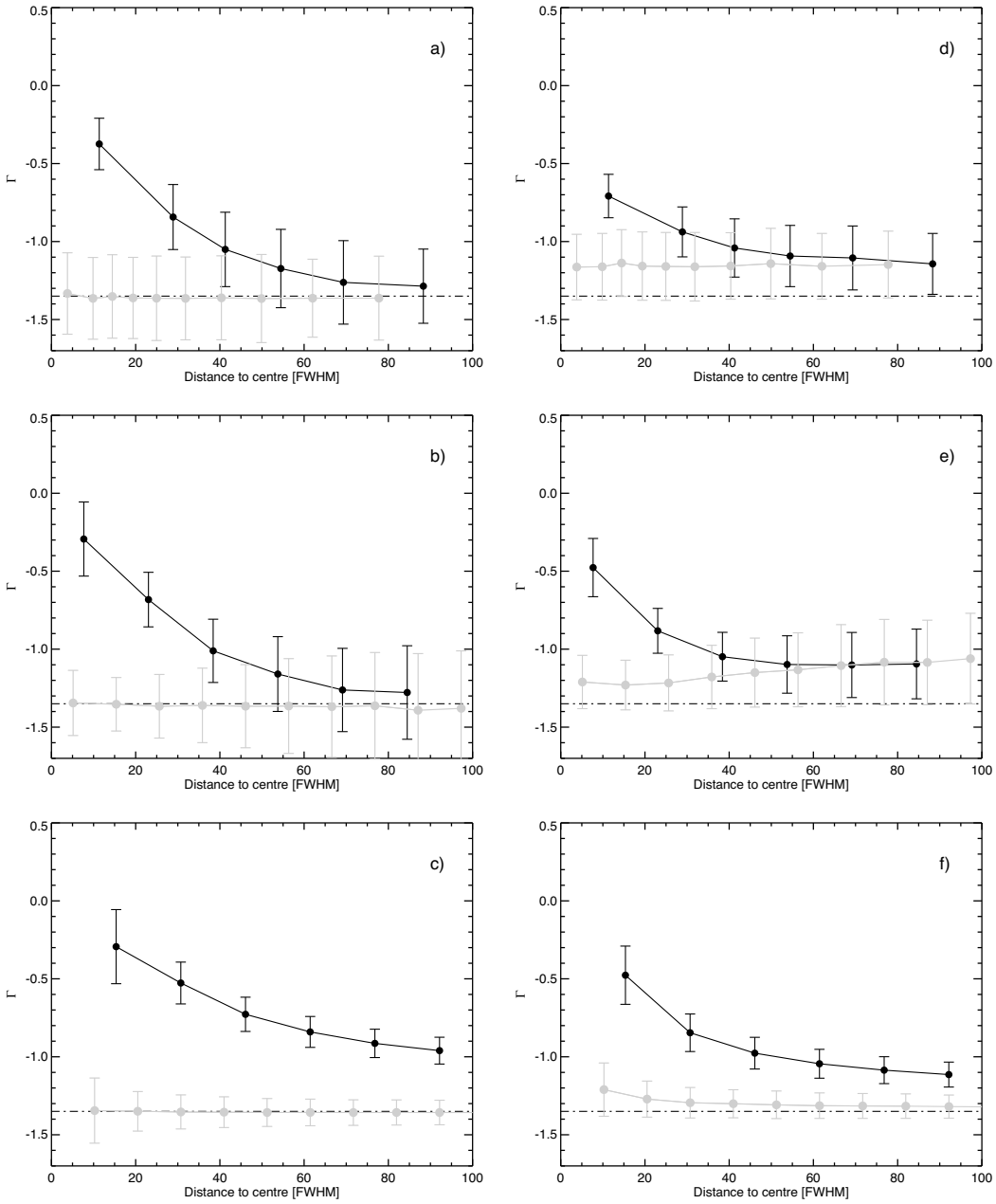

Fig. 4. Mass function slope (Γ) as a function of radius for the observed* clusters (*dark symbols*) when compared to the "true" clusters (*light symbols*). Panel **a)**: Γ is measured in equal-number (100 stars) radial annuli (the radii mark the centre of the annuli) and defining the mass functions such that all the mass bins have the same number of stars. Panel **b)**: Γ is measured in fixed-width (10 FWHM) radial annuli (the radii mark the centre of the annuli) and defining the mass function as in panel **a)**. Panel **c)**: Γ is measured in concentric circles (the radii mark the limits of the circles) and defining the mass function as in panel a). Panel **d)**: Γ is measured in equal-number (100 stars) radial annuli and defining the mass functions as fixed $\Delta \log(M/M_{\odot}) = 0.2$ histograms. Panel **e)**: Γ is measured in fixed-width (10 FWHM) radial annuli and defining the mass function as in panel **d)**. Panel **f)**: Γ is measured in concentric circles and defining the mass function as in panel **d)**. The profiles for the incomplete, observed* clusters mimic the effects of mass segregation.

the literature as evidence of mass segregation (Hillenbrand 1997; Stolte et al. 2006).

3.3. Mean mass

Following the same reasoning as before, the mean mass of a non-segregated cluster should be independent of the region where we choose to measure it. This is what we find when we plot the mean mass in concentric annuli for the synthetic clusters (Fig. 6, *light symbols*), regardless of using fixed-number (*left-hand panel*) or fixed-width (*right-hand panel*) rings.

Conversely, the observed* clusters (*dark symbols*) display a significant increase of the mean mass toward the cluster centre, as the faint stars in the centre are not as effectively detected as the massive stars, shifting the mean mass to higher values, a signature also often attributed to mass segregation.

3.4. Mean radius of the massive stars

In the present context we define the mean radius of any sample of stars as the mean distance of those stars to the centre of the cluster. For each cluster, we measured the mean radius of the

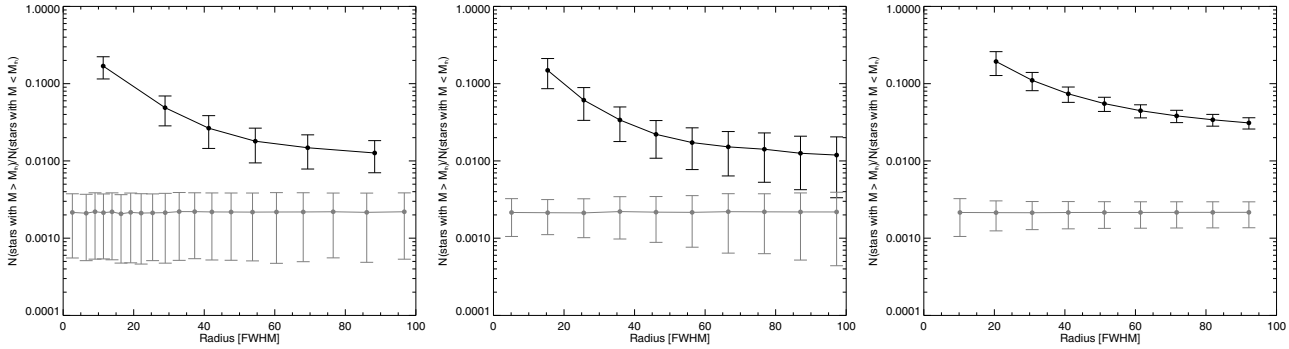

Fig. 5. Ratio of high- to low-mass stars with radius for a mass threshold of 10 $M_{\odot}$ for the "true" clusters (*light symbols*) and observed* clusters (*dark symbols*) measured in annuli of fixed number of stars (*left*), fixed-width annuli (*middle*) and concentric circles (*right*). The profiles for the incomplete, observed* clusters mimic the effects of mass segregation.

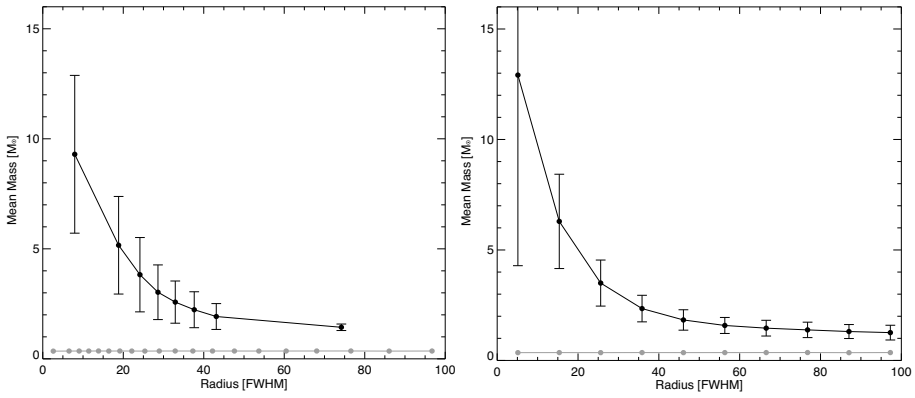

Fig. 6. Mean mass of the stars within annuli of equal number of stars (*left*) and fixed-width annuli (*right*) for the "true" (*light symbols*) and observed* (*dark symbols*) clusters.

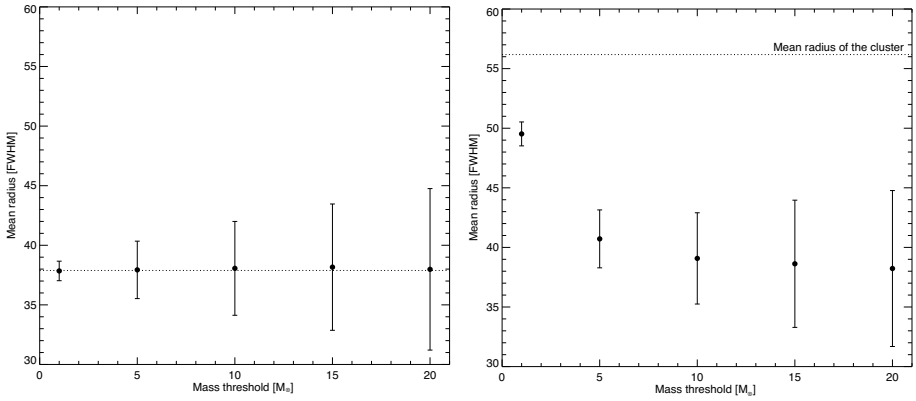

Fig. 7. Mean radius of the stars with masses higher than the designated mass threshold for the average of the 1000 "true" clusters (*left*) and for the observed* clusters (*right*). The *dotted* line represents the mean radius of the clusters.

massive stars and compared it to that of the cluster as a whole. The massive star subsample was defined using mass thresholds of 1, 5, 10, 15, and 20 $M_{\odot}$.

We find that both the mean radius of the "true" clusters and that of their massive stars have the same value for all mass thresholds (Fig. 7, *left*), although the cluster-to-cluster fluctuations increase with increasing threshold. This changes for the observed* clusters (*right-hand panel*), as the number of low-mass stars in the centre is significantly smaller than before due to crowding, causing the total mean radius of the cluster to become larger (56 FWHM), whereas the mean radius of the set of massive stars remains roughly the same for almost all mass thresholds, as these are not affected.

These profiles match those found in the literature (e.g., Sagar et al. 1988; Bonnell & Davies 1998; Schweizer 2004), where the authors consistently find the massive stars to have smaller mean radii when compared to the mean cluster radii.

4. On completeness corrections

In the previous sections we have shown that incompleteness due to crowding will mimic the effects of mass segregation in the commonly used indicators. This is so because they have the same effect: a depletion of low mass stars in the cluster core. The fundamental difference is that, whereas mass segregation in young clusters implies a physical process over which the stars of different masses are formed or somehow appear spatially segregated, crowding simply causes the observer to miss the low-mass stars due to the resolution limitation of the instrumental set-up. Many authors are aware of these limitations and apply more or less sophisticated completeness corrections to their samples, but how good are these corrections? Since we know in advance the exact composition of our synthetic clusters, we used one of them to perform a thorough investigation on the completeness assessment and correction process.

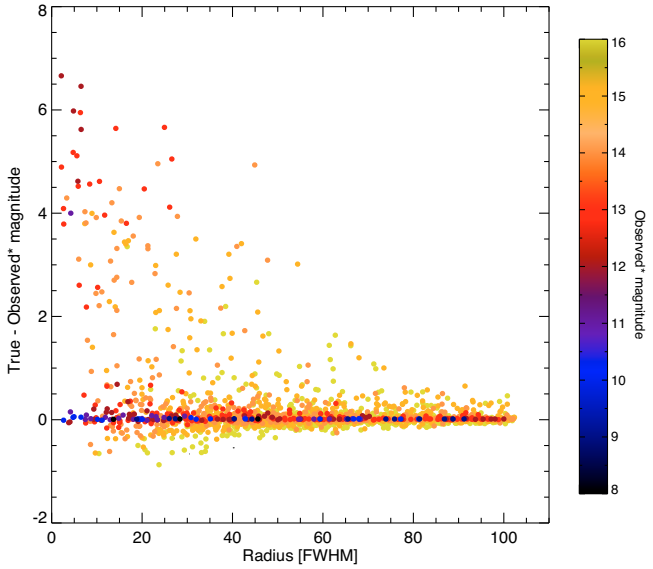

Fig. 8. Difference between the true and observed* brightness for the cluster stars as a function of distance to the centre. The colour-code maps the observed* brightness of the stars.

4.1. Completeness tests

The direct comparison of the true and observed* properties of a synthetic cluster is the most immediate way to gain insight into what is actually lost to observational limitations. Figure 8 shows the difference between the true and observed* brightness of cluster stars as a function of distance to the centre, while the colour-code maps the observed* brightness of the stars. It becomes clear that the two relevant consequences of crowding toward the cluster core are: (1) hampering source detection due to confusion caused by the close proximity of the sources; and (2) inflate the stars' brightness by blending their flux with that of unresolved neighbours. As a result, as we move into the centre of the cluster, we are less and less sensitive to the faint stars, and will tend to overestimate, sometimes by several magnitudes, the brightness of those we do detect. The bright stars, on the other hand, are equally detected everywhere throughout the cluster and their measured brightness is hardly affected by the crowding.

However insightful as this comparison may be, in real clusters we must rely on completeness tests to determine the extent to which we may trust the observations, as we lack the privileged information about the cluster's true composition. To address potential accuracy and reliability issues of completeness tests, we computed them for a synthetic cluster as if it were an actually observed image. For every 0.5 mag bin, we added artificial stars to the image in a grid such that each star is separated from its closest neighbour by two times the radius of the PSF +1 pixel. By forcing the artificial stars to be in such a grid we sampled the full extent of the cluster area without adding to the crowding. The images for each magnitude were then subject to source detection and photometry, and the output lists of sources were compared with the input grids. The completeness for magnitude $m_{\rm in}$ is then defined as the number of detected grid stars with measured magnitudes $m_{\rm out}$ that satisfy the condition $|m_{\rm in} - m_{\rm out}| < 0.1$, divided by the total number of stars of magnitude $m_{\rm in}$ in the input grid. The latter condition implies that an artificial star blended with a cluster star such that it affects its magnitude beyond the reasonable photometric uncertainty is rejected for completeness purposes, which happens very frequently in the crowded core, mainly for the faint stars. The outcome of these tests is therefore a high-fidelity completeness assessment that contains information, not only about the detection success rate, but also about how blending affects the incompleteness. We use the definition of completeness described above in the following sections.

4.2. Global completeness

The red solid line in Fig. 9 shows the global completeness – the fraction of artificial stars recovered with respect to the input stars in the grid – as a function of magnitude. These tests return a 90% global completeness for magnitude 12 (6.2 $M_{\odot}$ in our example). The *dotted line* is the *true* completeness defined here as the fraction of observed* cluster stars relative to the true number of stars for each magnitude in the synthetic cluster[1]. The local disparities between the two profiles are due to unresolved (blended) sources: whereas blending is excluded for the purpose of completeness tests (see Sect. 4.1), it does occur in observations – blended stars will appear in the list of observed* sources as single stars with good photometry. As a consequence, blended stars "leak" to different magnitude bins and cause the true completeness to be contaminated in an unpredictable way. For this reason, and again because the completeness tests include only single stars, the profiles fail to match for some magnitudes. Nevertheless, the overall agreement indicates that the accuracy of the global completeness tests is quite reasonable.

4.2.1. Correcting luminosity functions

An important and surprising corollary of the validation of global completeness tests above is that the global properties of the cluster, such as its mass function, can effectively be corrected for incompleteness due to crowding. Figure 10 shows the observed* (*solid line*), true (*dotted line*), and completeness corrected (*red diamonds*) luminosity functions for this cluster. The latter was derived by dividing the first by the completeness profile (*red line* in Fig. 9), and it is indeed very faithful to the true luminosity function for all but the last corrected bin, where the correction drops from 23% to 8%. The last reliable bin is four magnitudes fainter than the estimated 90% completeness limit (6.2 $M_{\odot}$), corresponding now to a mass of 0.3 $M_{\odot}$ in our example. This implies that one would, in principle, be able to see the first break of the mass function in this cluster even though the completeness limit is a great deal more massive.

This example shows the potential of the global completeness tests, but we emphasise that it is only valid for clusters with the same characteristics as the presented synthetic clusters, when crowding is the only source of incompleteness (e.g., no extinction), and for this particular method of evaluating completeness. Most completeness studies in the literature, although similar, are not as thorough as the one described here and must therefore be validated before extending this result to other degrees of crowding and/or observational configurations.

4.3. Radial completeness limitations

The global completeness discussed in the previous section describes the average behaviour in the whole cluster area, but is not representative of the cluster core where the crowding is most severe. The completeness tests described in Sect. 4.1 can then be analysed in concentric rings about the centre of the cluster to estimate the radial dependence of completeness. Figure 11 shows the completeness as a function of radius for the different magnitudes.

[1] Please refer to the last paragraph of Sect. 1 for a summary of the nomenclature and definitions used here.

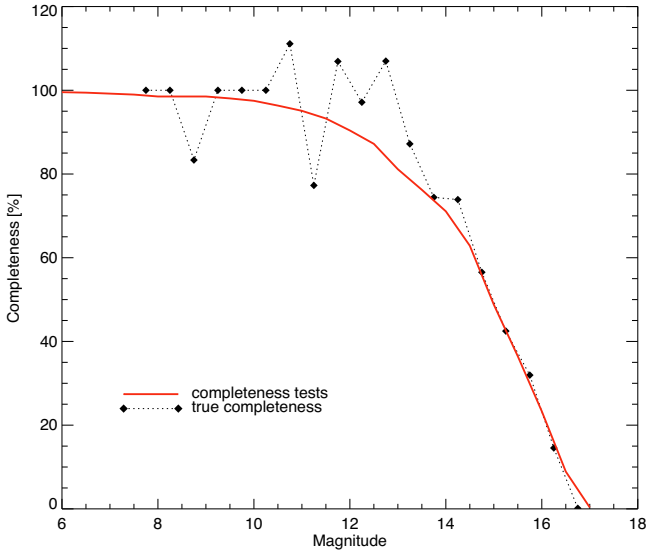

Fig. 9. Global completeness as a function of magnitude from the completeness tests (*red solid line*), and from direct comparison of the observed* and true brightnesses (*dotted line*).

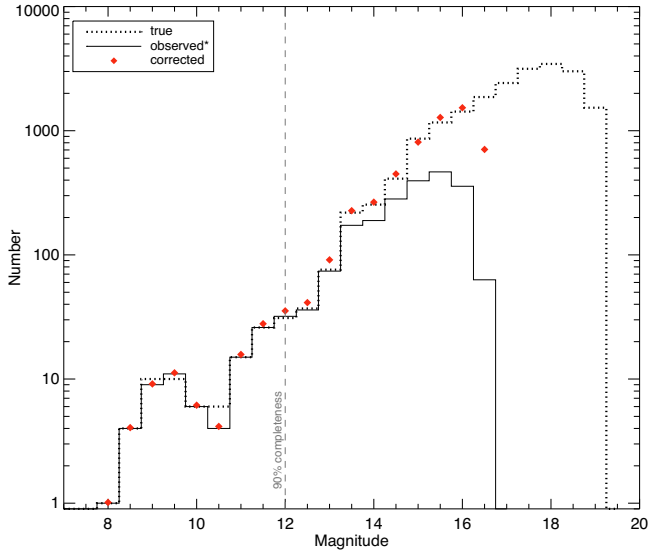

Fig. 10. Comparison of the observed* luminosity function (*solid line*) with the true (*dotted line*) and completeness corrected (*red diamonds*) luminosity functions.

Extrapolating from Fig. 9, one would trust these radial profiles to be a fair representation of the true radial completeness. However, when comparing both for any given magnitude we instead find a blunt disagreement (see Fig. 12 for magnitude 14). These differences are entirely attributable to the blending of unresolved sources: when selecting stars of magnitude m from the observed* list of sources to assess the true completeness, we include (blended) stars that are in reality fainter, while at the same time excluding true mth magnitude (blended) stars with inflated (combined) brightnesses. The consequence is that we appear to be more complete than what the grid completeness tests suggest simply because we cannot differentiate between blended and single sources.

In terms of completeness corrections, these "magnitude leaks" due to blending take much larger proportions than they did in the global completeness analysis (Sect. 4.2). On the global scale the effect of the magnitude leaks from the core is largely diluted, allowing for reasonable completeness corrections. Conversely, the radial completeness tests systematically imply very large (over-)corrections in the cluster core, which immediately produce a greatly inflated amount of stars, resulting in our case in an (over-)corrected cluster with typically 3.5 times more stars (up to magnitude 14) than the original synthetic cluster.

In terms of completeness assessment, both radial completeness estimates in Fig. 12 agree that: (1) the global completeness overestimates the completeness in the crowded central regions; and (2) that completeness is strongly radially dependent being more severe in the cluster core, which ultimately confirms the hypothesis that it is responsible for the apparent mass segregation.

To summarise, this analysis shows that there is a radial dependence of the completeness affecting primarily the low-mass stars that we cannot correct for, so no radial property (such as mass segregation) can be legitimately measured in the presence of severe crowding.

5. Conclusions

We used synthetic non-segregated, compact, and massive clusters to investigate the impact of the current approach to observational data on mass segregation studies. Our conclusion is that incompleteness due to crowding will produce the observed properties of mass segregated clusters, even when they are not segregated at all. Crowding causes the massive stars to be detected more effectively than the low-mass stars, resulting in an apparent depletion of low-mass stars in the cluster core, which then produces the characteristics typically attributed to mass segregation. More revealing, radial completeness tests provide erroneous estimates of the incompleteness and, as a consequence, lead to severe over-corrections. This is even more unsettling if we consider that it is not possible to evaluate the accuracy of the completeness determinations with the information from the observations alone. This is particularly critical for distant, rich clusters or clusters observed with poor spatial resolution or sensitivity.

We have also found that the way to present the data may furthermore influence the analysis, although to a much lesser extent. In what concerns the radial study of the mass function, it is imperative that the slope in each radial annulus be measured in mass bins with equal number of stars, as described in detail by Maíz Apellániz & Úbeda (2005). If this is so, then the radial binning will not influence the analysis. The other indicators (ratio of high- to low-mass stars and mean mass of the stars in annuli) are not affected by radial binning effects.

This exercise showed that the study of mass segregation cannot be dissociated from an exhaustive and rigorous study of completeness – which is not often found in the literature – and even then extreme caution must be exercised when interpreting radial properties as evidence of mass segregation.

The presence of interstellar extinction, not included in this analysis, will affect the mass segregation indicators in a more unpredictable way. On the one hand, the spatial distribution of dust can have all possible geometries, although it is expected that the massive stars in massive clusters will clear the dust from the cluster's core much more rapidly than they will the peripheries. On the other hand, the extinction will affect primordially the fainter, low-mass stars, again adding to the incompleteness effect and probably contribute, at least in their earlier stages, to aggravate the incompleteness problem on the cluster scale.

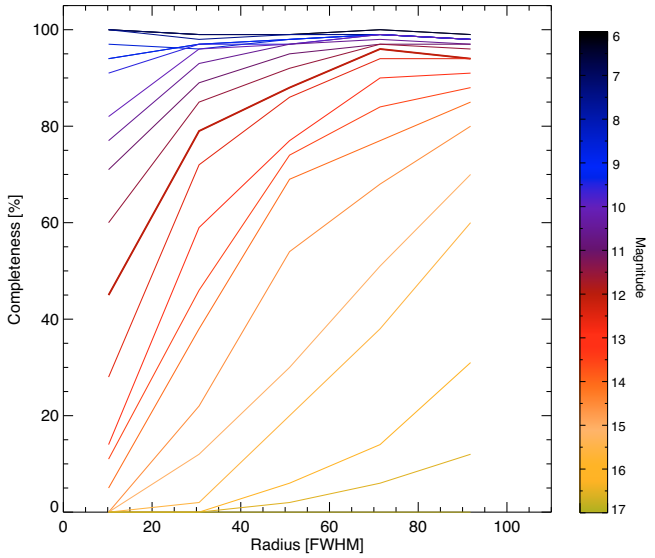

Fig. 11. Completeness tests as a function of radius for the different magnitudes. The line in bold indicates the 90% completeness limit determined in Sect. 4.2.

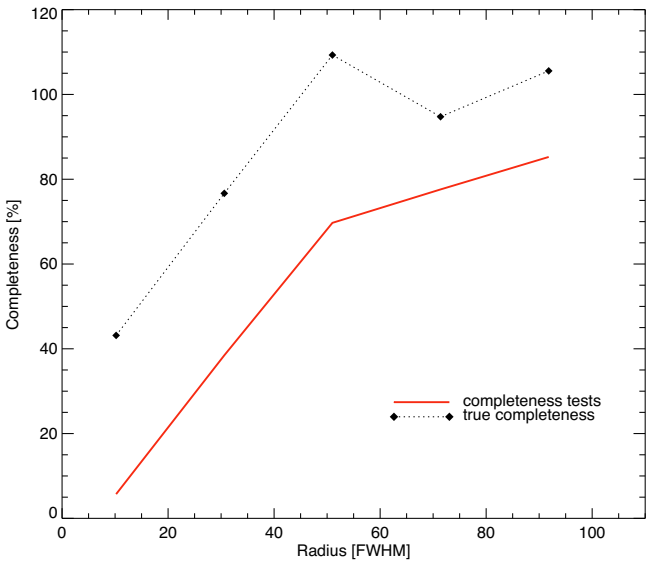

Fig. 12. Completeness as a function of radius from the completeness tests (*red solid line*), and from true completeness (*dotted line*) for magnitude 14.

An interesting outcome of the completeness analysis is that in some cases, such as in the one presented here of a massive cluster with no interstellar extinction, it may be reasonable to correct the global luminosity function – and, by extension, the mass function – for incompleteness, thus gaining information about fainter (low-mass) regimes that would otherwise be inaccessible, at least using the completeness tests we experimented with. Other tests may give different corrections and must be validated beforehand. This opens a safe, if not new, door to the study of the break of the IMF in massive galactic and extra-galactic clusters.

Acknowledgements. J. Ascenso acknowledges financial support from FCT, Portugal (grant SFRH/BD/13355/2003 and project POCTI/CFE-AST/55691/2004) and is grateful to the Calar Alto Observatory for hosting a very important part of the work. A special thanks also to Jarle Brinchmann and Prof. Pedro Lago for the helpful discussions of statistics. We also thank the anonymous referee for the constructive comments that contributed to improving this work.

References

Ascenso, J., Alves, J., Beletsky, Y., & Lago, M. T. V. T. 2007, A&A, 466, 137
Bica, E., & Bonatto, C. 2005, A&A, 443, 465
Binney, J., & Tremaine, S. 1987, Galactic dynamics (Princeton, NJ: Princeton University Press), 747
Bonatto, C., & Bica, E. 2005, A&A, 437, 483
Bonnell, I. A. 2000, in Stellar Clusters and Associations: Convection, Rotation, and Dynamos, ed. R. Pallavicini, G. Micela, & S. Sciortino, ASP Conf. Ser., 198, 161
Bonnell, I. A., & Davies, M. B. 1998, MNRAS, 295, 691
Brandl, B., Sams, B. J., Bertoldi, F., et al. 1996, ApJ, 466, 254
de Grijs, R., Gilmore, G. F., Johnson, R. A., & Mackey, A. D. 2002, MNRAS, 331, 245
Gouliermis, D., Keller, S. C., Kontizas, M., Kontizas, E., & Bellas-Velidis, I. 2004, A&A, 416, 137
Hillenbrand, L. A. 1997, AJ, 113, 1733
Hillenbrand, L. A., & Hartmann, L. W. 1998, ApJ, 492, 540
Jones, B. F., & Stauffer, J. R. 1991, AJ, 102, 1080
King, I. 1962, AJ, 67, 471
Kroupa, P. 2001, MNRAS, 322, 231
Maíz Apellániz, J., & Úbeda, L. 2005, ApJ, 629, 873
McNamara, B. J., & Sekiguchi, K. 1986, ApJ, 310, 613
Moitinho, A., Alfaro, E. J., Yun, J. L., & Phelps, R. L. 1997, AJ, 113, 1359
Sagar, R., Miakutin, V. I., Piskunov, A. E., & Dluzhnevskaia, O. B. 1988, MNRAS, 234, 831
Salpeter, E. E. 1955, ApJ, 121, 161
Schweizer, F. 2004, in The Formation and Evolution of Massive Young Star Clusters, ed. H. J. G. L. M. Lamers, L. J. Smith, & A. Nota, ASP Conf. Ser., 322, 111
Stolte, A., Grebel, E. K., Brandner, W., & Figer, D. F. 2002, A&A, 394, 459
Stolte, A., Brandner, W., Grebel, E. K., Lenzen, R., & Lagrange, A.-M. 2005, ApJ, 628, L113
Stolte, A., Brandner, W., Brandl, B., & Zinnecker, H. 2006, AJ, 132, 253
Tadross, A. L. 2005, Bull. Astron. Soc. India, 33, 421